Eur. Phys. J. B **31**, 151–157 (2003)
DOI: 10.1140/epjb/e2003-00019-5

THE EUROPEAN PHYSICAL JOURNAL B

# Low frequency transport measurements in $GdSr_2RuCu_2O_8$

A. Vecchione[1], D. Zola[2], G. Carapella[2], M. Gombos[1], S. Pace[2], G. Costabile[1], and C. Noce[1,a]

[1] Unità INFM di Salerno-Coherentia, Dipartimento di Fisica "E.R. Caianiello", Università di Salerno, 84081 Baronissi (Salerno), Italy
[2] Unità INFM di Salerno, Dipartimento di Fisica "E.R. Caianiello", Università di Salerno, 84081 Baronissi (Salerno), Italy

Received 18 September 2002
Published online 4 February 2003 – 

**Abstract.** Low frequency transport measurements are performed on $GdSr_2RuCu_2O_8$ pellets. The observed current-voltage curves are qualitatively explained in the framework of a simple phenomenological model accounting for coexistence in the sample of ferromagnetism and superconductivity. A Curie temperature $T_{cM} = 133$ K and a superconducting critical temperature $T_{cS} = 18$ K, with an onset temperature $T_{cO} = 33$ K, are extracted from the analysis of the current-voltage curves.

**PACS.** 74.50.+r Proximity effects, weak links, tunneling phenomena, and Josephson effects – 74.25.Ha Magnetic properties – 74.25.Nf Response to electromagnetic fields (nuclear magnetic resonance, surface impedance, etc.)

## 1 Introduction

The interplay of magnetism and superconductivity is a fundamental problem in condensed-matter physics and it has been studied experimentally and theoretically for almost four decades. These two cooperative phenomena are mutually antagonists. Indeed, the superconductivity is associated with the pairing of electrons states related to time reversal while in the magnetic states the time-reversal symmetry is lost and therefore there is a strong competition with superconductivity [1]. However, Schlabitz *et al.* [2] showed that surprisingly magnetism and superconductivity could coexist in the heavy fermion compound $URu_2Si_2$. Other heavy fermion superconductors have also been shown to exhibit magnetic moments in their superconducting phase [3]. All these compounds contain rare-earth or actinide ions with very localized $4f$ or $5f$ orbitals, strongly interacting with the conduction band electrons. This is in contrast to the Chevrel phases where magnetism and superconductivity coexist because the magnetic moments responsible for magnetism are only very weakly coupled with the electrons that form the condensate [4].

Nevertheless, there are been a number of recent studies reporting the coexistence of superconductivity and magnetic order in $R_{1.4}Ce_{0.6}Sr_2RuCu_2O_{10-\delta}$ [5] and $RSr_2RuCu_2O_8$ [6–8] where R = Gd, Eu. These latter compounds were originally synthesized by Bauernfeind *et al.* [9] and Felner and co-workers [10]. Most recent reports have focused on $GdSr_2RuCu_2O_8$, which has a unit cell similar to that of the $YBa_2Cu_3O_7$ high temperature cuprate, where there are two $CuO_2$ layers and one $RuO_2$ layer with the $CuO_2$ and $RuO_2$ layers being separated by insulating layers. Magnetization and muon spin rotation studies [7] have shown that there exists a magnetic ordering transition at temperature much greater than the superconducting transition temperature. Some studies have been interpreted in terms of ferromagnetic order arising from the Ru moment in the $RuO_2$ layers. This idea has generated considerable interest because ferromagnetic order and superconductivity are mutually competing processes and could only coexist *via* some accommodation of the respective order parameters by a spatial modulation [11] or *via* the formation of a spontaneous vortex phase [12]. However, powder neutron diffraction study [13] has shown that while there is a small ferromagnetic component, the low-field magnetic order is predominantly antiferromagnetic. These contrasting reports cast some doubt about the magnetic nature of this compound and at the present the situation has not been completely clarified. The aim of this paper is to give a contribution to this discussion. Indeed, we have found that transport measurements performed on $GdSr_2RuCu_2O_8$ sample are in agreement with predictions of a simple phenomenological model where *ferromagnetism* and superconductivity coexist. From the experimental results a Curie temperature $T_{cM} = 133$ K and a superconducting critical temperature $T_{cS} = 18$ K, with an onset temperature $T_{cO} = 33$ K, have been inferred.

The paper is organized as follows. In Section 2 the sample preparation is discussed. A phenomenological model for expected current-voltage curves is then given in Section 3. Experimental results are presented and discussed in

[a] e-mail: canio@sa.infn.it

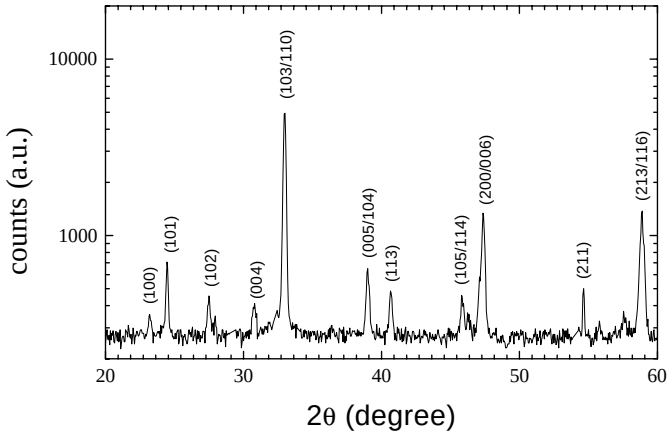


**Fig. 1.** (a) X-ray diffraction patterns of the $GdSr_2RuCu_2O_8$.

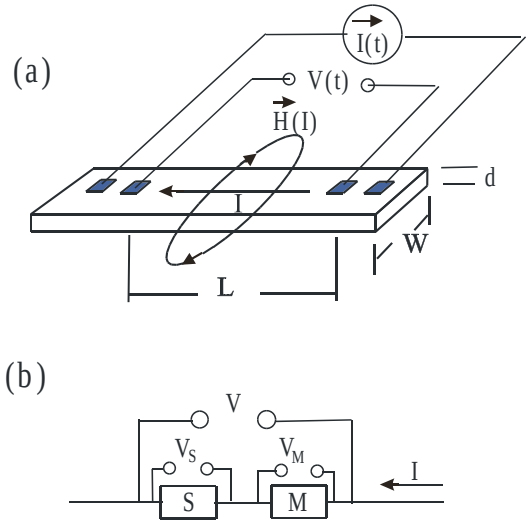


**Fig. 2.** (a) Sketch of wire connections used to measure the $GdSr_2RuCu_2O_8$ pellet. (b) Measured voltage is assumed to be the sum of two contributions. $V_M$ is associated to the magnetic phase and $V_S$ to the superconductive (or normal) phase.

connection with the theoretical prediction of the proposed model in Section 4. Some conclusions are finally given in the last section.

## 2 Sample preparation and characterization

Precursors powders have been synthesized starting from the pure binary oxide and carbonate powders, $Gd_2O_3$, $SrCO_3$, CuO, and $RuO_2$, mixed together in the proper amount and solid state reacted. The mixed powder was calcinated in air at 960 °C for 10 h. Annealing in flowing pure nitrogen at 1000 °C during 10 h was performed to reduce the formation of undesired phases such as $SrRuO_3$ [9].

Additional two steps of annealing of 10 h in pure flowing argon at 1020 °C also contributed to suppress the $SrRuO_3$ phase. Subsequently, the powders were oxygenated. Seven oxygenation cycles of a mean duration of 10 h, were performed at 1060 °C in flowing pure oxygen. These fully oxygenated powders were pressed in pellets by means of an hydrostatic press. Five 10 h cycles in pure oxygen flux, at temperatures of 1050 °C, 1055 °C, 1060 °C, 1065 °C, and 1070 °C, with intermediate grinding and mixing, have been performed on the pellets. Then, a last 90 h long cycle at 1070 °C and a refining one of 10 h at 1065 °C assured the complete oxygenation of the pellets. The crystal structure of the $GdSr_2RuCu_2O_8$ pellets was analyzed by X-ray powder diffraction method. The data were collected with a Philips PW-1700 powder diffractometer using Ni-filtered Cu K$\alpha$ radiation. The X-ray spectrum of a typical fully oxygenated pellet is shown in Figure 1. The scan pattern confirms that the sample is $GdSr_2RuCu_2O_8$ single phased.

## 3 Expected ac current-voltage curves

If a magnetic phase is present in the $GdSr_2RuCu_2O_8$, an hysteretic current-voltage ($I-V$) curve should be expected when the current is swept with a frequency $\omega$. In transport measurements, the four contact wire connection sketched in Figure 2a is typically used. Here, the forcing current $I(t)$ generates a magnetic field $\mathbf{H}(t)$=$\mathbf{H}[I(t)]$ with an associated magnetic induction $\mathbf{B}(t)$=$\mathbf{B}[\mathbf{H}(t)]$. At first order, the magnetic field depends linearly on the forcing current, $H(t) \propto I(t)$, so that $B(t) = B[I(t)]$ is too. From Maxwell equations, we expect a voltage drop contribution due to the temporal derivative of the magnetic flux linked to the voltage wires. However, such a contribution is relevant only if the magnetic induction field is quite high, *i.e.* if magnetic phases are involved. The $GdSr_2RuCu_2O_8$ can be phenomenologically seen as a series connection of superconducting and magnetic layers. Hence, we expect the measured total voltage to be the sum of a superconducting contribution $V_S$ and a magnetic contribution $V_M$ (see Fig. 2b):

$$V = V_S + V_M$$

$$V_M = \frac{\mathrm{d}\Phi[B]}{\mathrm{d}t} \propto \frac{\mathrm{d}B(t)}{\mathrm{d}t} = \frac{\mathrm{d}B[I(t)]}{\mathrm{d}t}$$

where we assumed that the relevant inductive voltage is essentially due to the magnetic component. Some qualitative predictions of the $I-V_M$ characteristic are possible from an analysis of the expected $B[I(t)]$.

Generally, $\mathbf{B}$ is a nonlinear function of $\mathbf{H}$ when a material is in a magnetic phase. In the following we are concerned with low magnetic field (forcing current) amplitudes. In such a case, a linear relationship between $\mathbf{B}$ and $\mathbf{H}$ can be assumed for the paramagnetic phase. Due to the vanishingly small net magnetization, for an antiferromagnetic phase an approximatively linear $B(H)$ relation could be again inferred, while a nonlinear relation should be expected for a strongly ordered phase as the ferromagnetic one. The last case can be qualitatively discussed as follows. At a given low amplitude magnetic field, a linear relation between $\mathbf{B}$ and $\mathbf{H}$ (see Fig. 3a) can be expected for

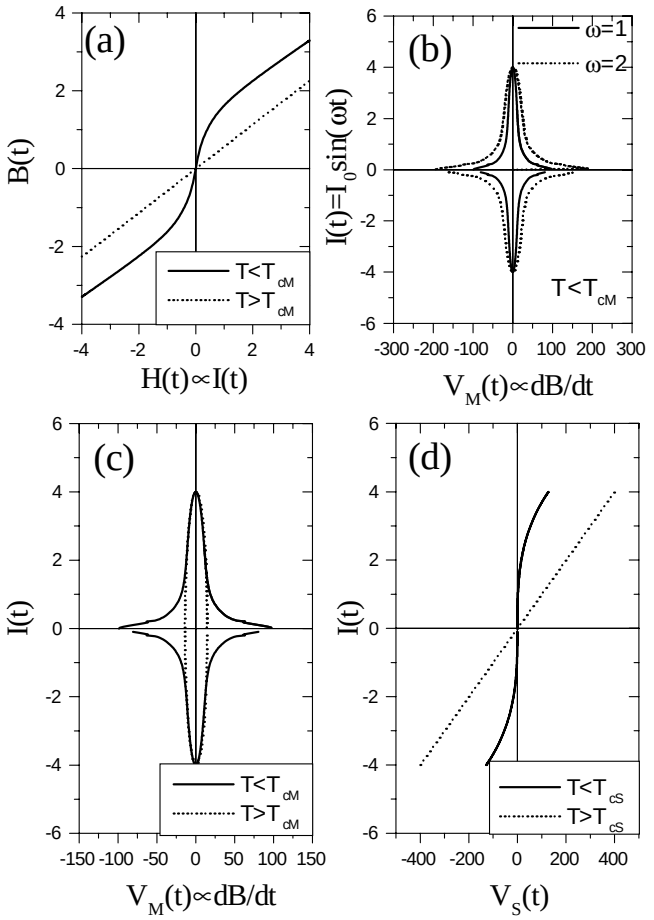


**Fig. 3.** (a) Low magnetic field approximation of $B(H)$ for the ferromagnetic phase ($T < T_{cM}$) and the paramagnetic phase ($T > T_{cM}$). (b) $I - V_M$ curves of the ferromagnetic phase for two different pulsations of a sinusoidal current forcing. (c) The shape of ac $I - V_M$ curves is truly elliptical for the paramagnetic phase and becomes a distorted ellipse in the ferromagnetic phase. (d) Typical $I - V_S$ curves of the superconductive ($T < T_{cS}$) or resistive ($T > T_{cS}$) phases.

temperatures above the ferromagnetic transition temperature $T_{cM}$ (*i.e.* when the material is in the paramagnetic phase) while a strongly nonlinear relation between **B** and **H** should be expected for temperatures below $T_{cM}$ (*i.e.* when the material is in the ferromagnetic phase). Due to the very low magnetic fields we can generate with the normally used forcing currents (of the order of some mA) we can assume that the saturation field will never reached when the material is in the ferromagnetic phase. In other words, for the used currents only the virgin curve of the hysteresis loop will be normally swept, so that a single-valued functional form $B(t) = B[I(t)]$ similar to the one shown in Figure 3a can be expected to approximately describe the material in the ferromagnetic phase. In such a limit, for a sinusoidal forcing current of amplitude $I_0$ and pulsation $\omega$ the $I - V_M$ curves shown in Figure 3b should be observed for the ferromagnetic phase. Moreover, the distorted ellipse typical of the ferromagnetic phase (at

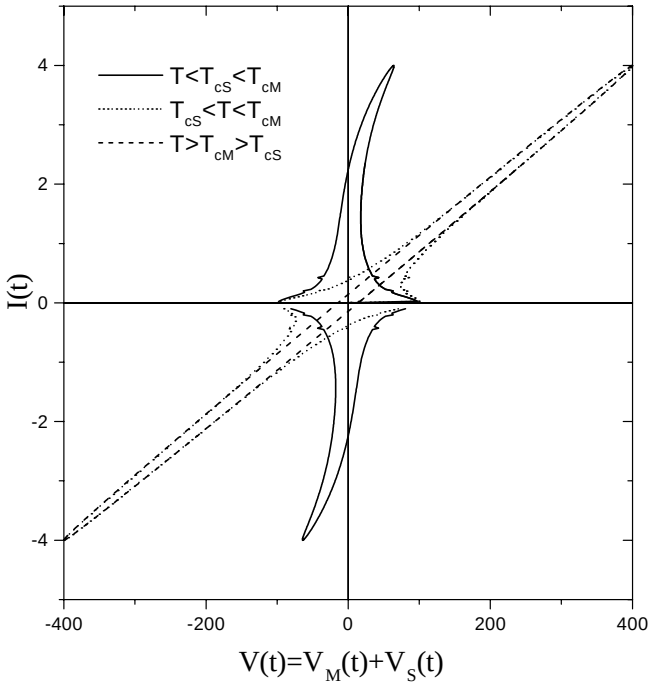


**Fig. 4.** Total ac current-voltage curve predicted for $GdSr_2RuCu_2O_8$ pellet at three relevant temperatures.

$T < T_{cM}$) should become a pure ellipse in the paramagnetic phase (at $T > T_{cM}$), as shown in Figure 3c.

Referring to the superconducting phase, the standard ac $I - V_S$ curves schematically plotted in Figure 3d are expected for temperatures below or above the superconducting transition temperature $T_{cS}$. For $T < T_{cS}$ is $V_S = 0$ for amplitude of the forcing current lower than a critical current value $I_c$, while a truly resistive curve is observed for $T > T_{cS}$. As stated above, the measured voltage of $GdSr_2RuCu_2O_8$ pellet is $V = V_M + V_S$. Hence, from information in Figures 3c and d, the expected ac $I - V$ curves should look similar to the ones we plotted in Figure 4 for three relevant temperatures. We should remark that, if observed, the peculiar outward cusp-like distortion of the $I - V$ curve around $I = 0$ is a signature of a ferromagnetic order originating from the strong nonlinear increase of the magnetic susceptibility below the Curie temperature. Conversely, for an antiferromagnetic order, a smoother distortion of the $I - V$ curve should be expected, and the area of the ellipse of the paramagnetic phase should decrease for temperatures below the Néel temperature due to the decrease of the magnetic susceptibility of the antiferromagnetic phase when the temperature is lowered.

## 4 Transport measurements and discussion

Measurements of $I-V$ curves were performed on a slice of $GdSr_2RuCu_2O_8$ using the four contact technique shown in Figure 2a. The sizes of the slice were $L = 5$ mm, $W = 2$ mm, and $d = 0.7$ mm. A sinusoidal forcing current ranging from 4 mA to 6 mA and frequency values of 10, 20

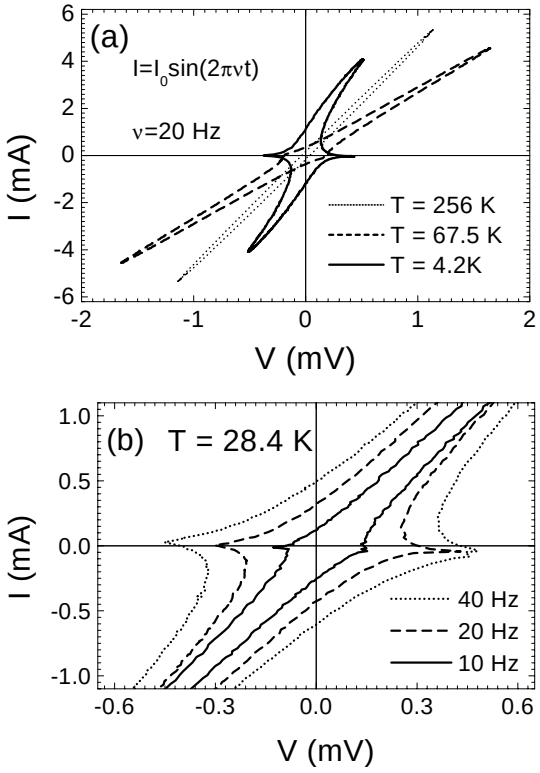


**Fig. 5.** (a) Experimental $I - V$ curves measured at three different temperatures. The frequency of current supply was 20 Hz. (b) $I - V$ curves measured at $T = 28.4$ K at different frequencies

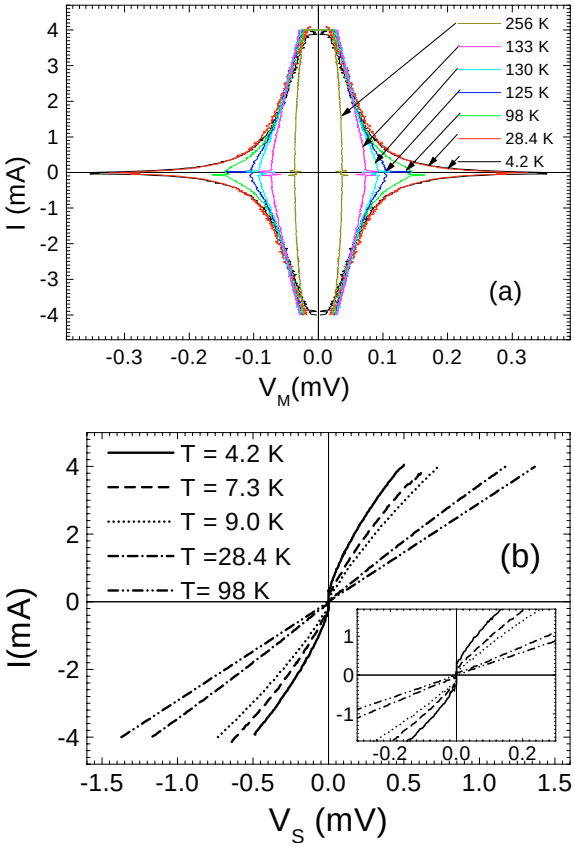


**Fig. 6.** Irreversible (a) and reversible (b) component extracted by experimental $I - V$ curves.

and 40 Hz were used. In order to reduce external electromagnetic interference, measurements were performed in a shielded room. The sample was also enclosed in a cryoperm shield to minimize external spurious magnetic field.

In Figure 5a, $I - V$ curves recorded at three different temperatures are shown. At first sight, the curves are in qualitative agreement with the calculated ones (see Fig. 4), resulting from the phenomenological model reported in the previous section. The $I - V$ curves show an hysteretic behavior at each temperature measured. Below a certain temperature, an outward cusp-like distortion of the elliptical shape at $T = 256$ K is evident in the curves. Moreover, the loop area always increases when temperature is lowered. As stated in the previous section this means that a *ferromagnetic* phase is involved in the material.

Figure 5b shows that the loop area increases with the frequency of the current sweep, as expected for an inductive (magnetic) contribution $V_M \propto \mathrm{d}B/\mathrm{d}t$ to the total voltage drop. The increase of the impedance with the frequency of the forcing current rule out the possibility of a capacitive coupling due, for example, to bad wire connections on the sample. In fact, for a capacitive coupling an impedance decreasing with frequency of forcing current should be observed. By comparison of Figures 5b and 3b, we deduce that a voltage contribution from a ferromagnetic phase is achieved. In the previous section, we have assumed that the electrical response of the material can be described as the series connection of a normal (superconducting/resistive) phase and a magnetic (ferromagnetic/paramagnetic) phase. When the material is a.c. supplied, the resistive (normal) component gives a reversible voltage signal, whereas the inductive (magnetic) one gives rise to an irreversible response accounting for the hysteretic shape of the voltage-current curves in the $I - V$ plane. In order to study separately the resistive and the inductive components of the measured $I - V$ curves, the reversible ($V_S$) and the irreversible ($V_M$) voltage were extracted in each curve. The reversible component in the total voltage signal, was calculated by using the simple formula

$$V_S(I) = \frac{V_{up}(I) + V_{dw}(I)}{2} \tag{1}$$

where $V_{up}$ and $V_{dw}$ are respectively the voltage values measured during the increasing and the decreasing branch of the sinusoidal forcing current. Then, the irreversible component was extracted according to

$$V_M(I) = V(I) - V_S(I). \tag{2}$$

The irreversible part extracted from the total signal measured is shown in Figure 6a. Again, a qualitative agreement with the computed curves (see Fig. 3b) is recognized. For temperatures ranging from 4.2 K up to about 70 K, the loop area diminishes very slowly. Then the area

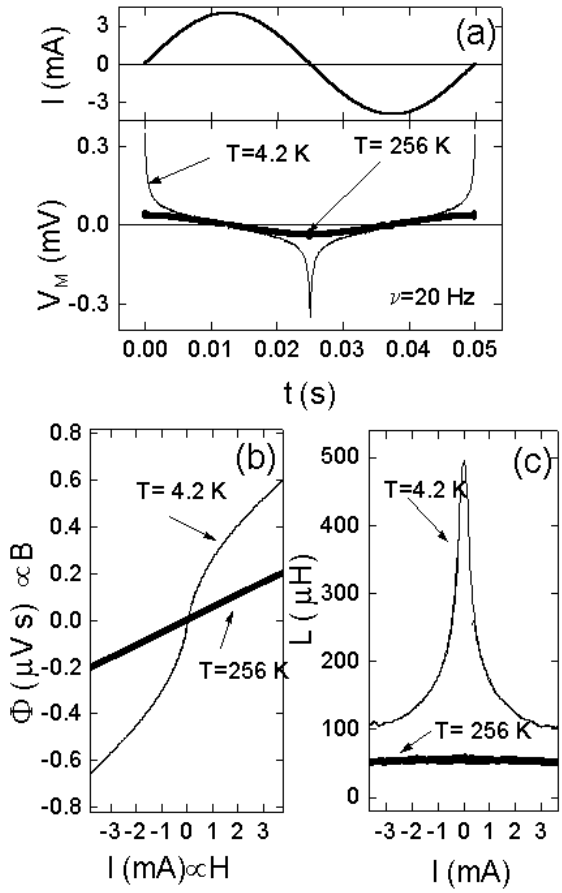


**Fig. 7.** (a) Distortion of voltage waveforms in the paramagnetic and in the ferromagnetic phase, as extracted from the irreversible $I - V_M$ curves in Figure 6a. Deduced flux-current (b) and Inductance-current (c) relations for paramagnetic ($T = 256$ K) and ferromagnetic ($T = 4.2$ K) phases.

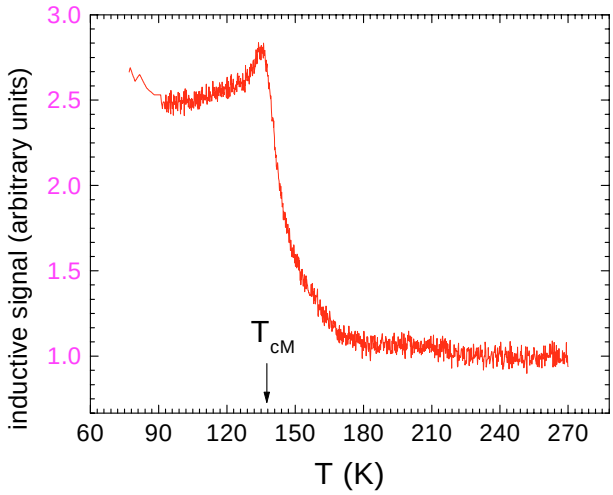


**Fig. 8.** Inductive signal (proportional to mean magnetic permeability) as a function of the temperature, around the Ferromagnetic/Paramagnetic transition of the sample.

decreases quickly and smoothly changes shape becoming elliptical around $T_{cM} = 133$ K. From analysis of the previous section we identify $T_{cM} = 133$ K as the Curie transition temperature of the magnetic phase in the sample. In Figure 6b the reversible curves, ascribed to the resistive share in the total voltage signal, are shown for different temperatures. The typical non linear $I - V$ for a superconductor ($V_S = 0$ for $-Ic < I < Ic$) can be recognized for temperatures below $T_{cS} = 18$ K while linear behavior is recovered above this temperature.

From data of the irreversible curve, some information can be deduced to check the self-consistence of our model. For the sake of clarity, we refer to the paramagnetic curve achieved at $T = 256$ K and to the ferromagnetic curve achieved at $T = 4.2$ K in Figure 6a. In Figure 7a we show both the forcing current and the measured voltages corresponding to these two relevant temperatures. As it is seen, the voltage signal is simply dephased (of $\pi/2$) from the current signal at $T = 256$ K, accounting for a linear inductive response in the paramagnetic phase, while it is dephased and distorted at $T = 4.2$ K, accounting for some quite non-linear inductive response in the ferromagnetic phase. Recalling that $V_M(t) = \mathrm{d}\Phi/\mathrm{d}t$, the magnetic flux as a function of the forcing current can be deduced from voltages $V_M(t)$. In Figure 7b the flux-current relations of the paramagnetic and ferromagnetic phases calculated by data in Figure 7a are shown. By noticing that the flux is proportional to the magnetic induction $B$ and that the current is proportional to the applied magnetic field $H$, the curves in Figure 7b also describe the functional $B(H)$ dependence, as extracted from experimental data. A comparison of Figure 7b with Figure 3a shows that our initial assumption for $B(H)$ curves is quite consistent with the $B(H)$ relations extracted from the experimental data. This corroborates the self-consistence of the approach we followed. From $\Phi(I)$ relations in Figure 7b the inductances $L(I) = \mathrm{d}\Phi(I)/\mathrm{d}I$ shown in Figure 7c can be estimated. The strongly nonlinear inductance expected for a ferromagnetic phase is recovered at $T = 4.2$ K. The estimated self-inductances are found quite large, but not so different from the ones normally achieved for ceramic ferrites. From estimated inductances a quantitative analysis of magnetic permeability or susceptibility could be done, passing from an accurate estimation of geometrical parameters. However, this is beyond the aim of the present work. The aim of the present work is to account for measured ac current-voltage characteristic alone. Magnetic response study, is obviously, better made with ordinary and well established techniques. We used standard inductive method to independently estimate the magnetic transition temperature in our sample. As seen in Figure 8, the inductive method gives a Curie temperature $T_{cM} \approx 133$ K, in agreement with the estimate we extracted from analysis of the irreversible component of current-voltage curves.

From data of the reversible curve, we extracted the resistance as a function of the temperature shown in Figure 9. The temperature $T_{cS}$, corresponding to a full superconducting phase in the sample ($V_S = 0$) and the onset temperature $T_{cO}$ were estimated 18 K and 33 K, respectively. In our measurements the non-linear behavior

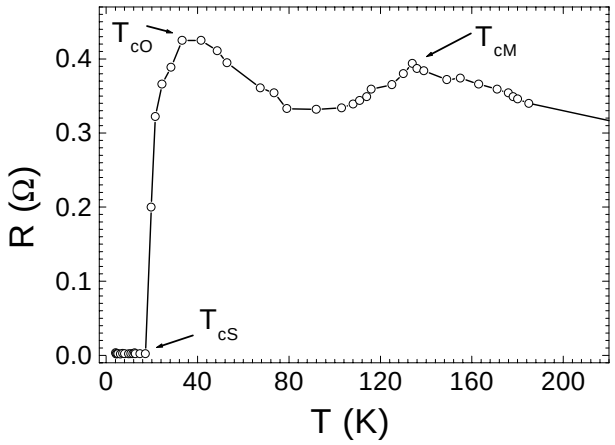


**Fig. 9.** Resistance *versus* temperature calculated by using the reversible $I - V$ curves.

in reversible $I - V$ curves, can be recognized up to 18 K. Increasing the temperature from $T_{cS}$ up to $T_{cO}$ the reversible $I - V$ curves are linear with a quite fast increase of the resistivity. Above $T_{cO}$, the measured resistance get lower and for $T_{cM} = 133$ K the resistance shows a peak. For temperatures above the magnetic transition temperature the resistance diminishes again. The observed behavior agrees with resistivity data measured with ordinary approach reported in the literature for this material.

Two main results can be drawn from the data above presented.

Firstly, we find a clear evidence of changes near 130 K of irreversible and reversible components of the $I - V$ curves and therefore we infer that they could be ascribed to a ferromagnetic/paramagnetic-like transition. This speculation agrees well with the results reported in literature that find a magnetic ordering temperature at around 130 K [6]. The appearance of a spontaneous magnetic moment below this temperature at a very low field suggests that the transition at $T_{cM}$ must have a significant ferromagnetic component. The experimental results also suggest that the ferromagnetic component persists to the lowest measured temperature attained in the experiments and does not appear to weaken when the superconductivity comes in at $T_{cO} = 33$ K. The existence of a ferromagnetic component in the superconducting state of this sample suggested by the low frequency data here presented, is also supported by magnetic measurements performed on the same sample and reported elsewhere [14]. Moreover, because no impurity lines were detected in the X-ray diffraction pattern within the experimental resolution we may argue that no extra phases are responsible for ferromagnetism implying that this ordering is due to an intrinsic phase and in this respect we could infer that the coexistence of superconductivity and ferromagnetism is realized within a microscopic scale. This hypothesis is corroborated by magneto-optical-imaging measurements where ferromagnetism and superconductivity are directly observed to coexist in the same space within the experimental resolution [15].

Second, we speculate briefly on the significance of the phenomenological model previously introduced. Within our model, we assume that the measured total voltage is the sum of two contributions: one coming from the superconducting channel and the other due to the ferromagnetic ordering. Although the crudeness of the assumptions, we have been able to reproduce fairly the shape of the $I - V$ curves and more importantly we clearly identify the superconducting contribution only when the ferromagnetic one is subtracted. This contribution is of the standard form for a generic superconductor and this in turn further supports the correctness of our assumptions.

## 5 Conclusion

In conclusion, we performed measurements on $GdSr_2RuCu_2O_8$ ruthenate-cuprate with the aim to address the question of the nature of the magnetic order in the superconducting phase and trying to improve the understanding of the physics of ruthenate-cuprate materials. We used a relatively inexplored approach, based on the analysis of low frequency electrical transport measurements. The observed current-voltage curves have been found in quite good qualitative agreement with the predictions of a phenomenological model accounting for coexistence of both magnetic and superconducting phases in the sample. Our experimental results suggest that $GdSr_2RuCu_2O_8$ is paramagnetic above $T_{cM} = 133$ K, ferromagnetic between $T_{cS} = 18$ K and $T_{cM} = 133$ K, and both ferromagnetic and superconducting below $T_{cS} = 18$ K.

We want to stress that at the moment there is not a general consensus about the magnetic nature of this compound. The first measurements indicated ferromagnetic ordering of Ru moments at $T_{cM} = 133$ K [7]. The attempt to observe ferromagnetic ordering using neutron diffraction in $^{160}$Gd enriched samples was unsuccessful [16], then extra peaks corresponding to a doubled unit cell ascribed to the antiferromagnetic ordering of the Ru moments in a G-type arrangement have been detected [13]. Recent X-ray absorption near-edge structure experiments indicate that there is a mixture of pentavalent and tetravalent Ru ions in $GdSr_2RuCu_2O_8$ showing that a critical reinterpretation of magnetic data is necessary [17]. Indeed, due to the mixed valence nature of Ru within Gd1212 compound, some kind of charge ordering may be responsible for the observed doubled unit cell [18]. In our measurements the area of the ellipse of the paramagnetic phase does not decrease when the temperature is lowered below $T_{cM}$ and this result in turn suggests that the antiferromagnetic phase is not observed in our sample within our approach. For completeness, we point out that we cannot exclude the presence of an antiferromagnetic phase since in our measurements the ferromagnetic effects are certainly more robust and should hide the antiferromagnetic ones.

We gratefully acknowledge the contribution of D. Sisti in the sample preparation and the assistance of R. Ciancio in the inductive measurements.

## References


1. M.B. Maple, Physica B **215**, 110 (1995)
2. W. Schlabitz *et al.*, Z. Phys. B **62**, 171 (1986)
3. A. Amato, Rev. Mod. Phys. **69**, 1119 (1997)
4. Ø. Fischer, Appl. Phys. **16**, 1 (1978)
5. I. Felner, U. Asaf, O. Millo, Phys. Rev. B **55**, R3374 (1997)
6. J. Tallon *et al.*, IEEE Trans. Appl. Supercond. **9**, 1051 (1999)
7. C. Bernhard *et al.*, Phys. Rev. B **59**, 14099 (1999)
8. G.V.M. Williams, S. Krämer, Phys. Rev. B **62**, 4132 (2000)
9. L. Bauernfeind, W. Widder, H.F. Braun, Physica C **254**, 151 (1995); L. Bauernfeind, W. Widder, H.F. Braun, J. Low Temp. Phys. **105**, 1605 (1996)
10. I. Felner, U. Asaf, S. Reich, Y. Tsabba, Physica C **311**, 163 (1999)
11. C.W. Chu *et al.*, Physica C **335**, 231 (2000)
12. E.B. Sonin, I. Felner, Phys. Rev. B **57**, 14000 (1998); I. Felner, U. Asaf, Y. Levi, O. Millo, Physica C **334**, 141 (2000)
13. J.W. Lynn *et al.*, Phys. Rev. B **61**, 14964 (2000)
14. A. Vecchione *et al.*, Physica C **372-376**, 1229 (2002)
15. C.W. Chu *et al.*, `cond-mat/9910056`
16. O. Chmaissen *et al.*, Phys. Rev. B **61**, 6401 (2000)
17. R.S. Liu *et al.*, Phys. Rev. B **63**, 212507 (2001)
18. A. Butera *et al.*, Phys. Rev. B **63**, 054442 (2001)